# Faculty Scholarship Collection



| | |
|---|---|
| Article Title | Solubility considerations in relative block crystallization and morphology of PEO-b-PCL films |
| Author(s) | Tower, Cole W.; Allen, Kristi; Carandang, Allison; Van Horn, Ryan M. |
| Allegheny Faculty Author(s) | Van Horn, Ryan M. |
| Journal Title | *Polymer Crystallization* |
| Citation | Tower, CW, Allen, K, Carandang, A, Van Horn, RM. Solubility considerations in relative block crystallization and morphology of PEO-b-PCL films. Polymer Crystallization. 2020; 3:e10107. https://doi.org/10.1002/pcr2.10107 |
| DOI | 10.1002/pcr2.10107 |
| Link to article on publisher's website | https://onlinelibrary.wiley.com/doi/am-pdf/10.1002/pcr2.10107 (Author Manuscript [postprint]) |

Van Horn Ryan M (Orcid ID: 0000-0002-1065-7378)

# Solubility Considerations in Relative Block Crystallization and Morphology of PEO-*b*-PCL Films

**Cole W. Tower,[1] Kristi Allen,[1] Allison Carandang,[1] and Ryan M. Van Horn[1,2]**

[1]Department of Chemistry, Allegheny College, Meadville, PA 16335, USA

[2]Department of Chemical and Biomolecular Engineering, Lafayette College, Easton, PA 18042, USA

Correspondence to: Ryan M. Van Horn (E-mail: *vanhorrm@lafayette.edu*)

Additional Supporting Information may be found in the online version of this article.

**ABSTRACT**

Poly(ethylene oxide)-*block*-poly(ε-caprolactone) (PEO-*b*-PCL) is a heavily investigated amphiphilic crystalline-crystalline diblock copolymer. Its macroscopic physical properties are influenced by the crystallization behavior, which is robust due to similar crystallization temperatures of PEO and PCL. As such, tailoring the crystallinity and crystalline morphology should be advantageous to achieving desired changes in film properties. One method to manipulate the crystallization, analyzed here, is the selective solvation of one block during solvent casting. By careful solvent selection, the crystallization of PEO and PCL during solvent evaporation led to changes in relative crystallinity and film morphology. The effect of environmental humidity on the crystallization mechanism and relative block crystallization was explored in detail using FTIR.

## INTRODUCTION

Block copolymers have been a topic of great interest due to their ability to be widely tuned by their preparation conditions such as solvent interactions and thermal history. Block copolymers promise contribution to a growing variety of biomedical applications including sutures, tissue scaffolds,[1] and drug delivery.[2-5] Block copolymers are particularly of interest due to their ability to combine the properties of two or more homopolymers and their hierarchical structure to better tailor the material to a desired application.

Poly(ethylene oxide) (PEO) and poly(ε-caprolactone) (PCL) are widely used in the biomaterials industry. PCL is hydrophobic, is biocompatible,[6-8] and can degrade both hydrolytically[6-8] and enzymatically,[9-10] adding to its potential in various drug delivery methods. PCL has high drug permeability, but is limited in its drug delivery potential due to its excessive degradation time resulting from its high crystallinity and hydrophobicity.[6] PEO is hydrophilic, biocompatible, and non-degradable by hydrolysis. PEO's water solubility makes PEO homopolymer less suitable for controlled drug delivery applications. A viable solution to maintain desirable characteristic properties while minimizing the disadvantages of each homopolymer is utilizing the block copolymer, PEO-*b*-PCL. PEO-*b*-PCL remains biodegradable

This is the author manuscript accepted for publication and has undergone full peer review but has not been through the copyediting, typesetting, pagination and proofreading process, which may lead to differences between this version and the Version of Record. Please cite this article as doi: 10.1002/pcr2.10107

and biocompatible; however, it is amphiphilic, relatively strong, and allows for broader and more controlled degradation properties.[11]

Each block of a copolymer can be either amorphous or semi-crystalline, resulting in three possibilities for diblock copolymers: crystalline-crystalline, amorphous-amorphous, or amorphous-crystalline.[12-14] Much research has been done on crystallization of amorphous-crystalline block copolymers, and an increasing amount is being done on the comparatively complicated crystallization processes of crystalline-crystalline block copolymers.[12]

Fundamental understanding of crystallinity and the crystallization process in crystalline-crystalline block copolymers is essential in tailoring them for a specific use. Drug permeability,[15] biodegradability,[6,16] and mechanical properties of polymer films depend heavily on crystallinity. The block crystallization order determines the macromolecular structure[12,14] and much of the properties of the end material. Relative block melting temperature ($T_m$),[12] relative block molecular weight or weight fraction ($w_{block}$),[17-20] and solvent interaction[21-22] are some factors that affect block crystallization. PEO-*b*-PCL block copolymer crystallization has been studied extensively (see, for example, Refs. 21-34) because PEO and PCL homopolymer $T_m$s are similar.

PEO-*b*-PCL copolymers can have differing crystallization mechanisms because the melting and crystallization temperatures for each block are similar. Sequential block crystallization occurs in crystalline-crystalline block copolymer systems where the difference in melting point between the two blocks is large or when block asymmetry is high. A sequential block crystallization mechanism is defined by the start and finish of the crystallization of the first nucleating block, and the crystallization of the second block begins only when the material is cooled to lower temperatures (larger undercooling, $\Delta T$). The block with the higher $T_m$ (higher crystallization temperature, $T_x$) or the larger weight fraction will crystallize first,[12] followed by the pseudo-confined crystallization of the lower $T_x$ or minority block. Coincident block crystallization mechanisms occur in systems where the melting temperature of the two blocks is similar, and the blocks are symmetrical.[17-21] Here, it is possible to control which block crystallizes first by providing favorable crystallization conditions for one block or the other.[21-22] Therefore, it is possible to create films with different structure and properties from the same parent material by altering simple experimental conditions such as casting solvent and temperature.

In both coincident and sequential crystallization of weakly-segregated or miscible block copolymers, like PEO-*b*-PCL, the first block that crystalizes creates a spherulitic structure with lamella growing radially between which the crystallization of the second block is confined. Because of the covalent bond between the two blocks, the second block is forced to crystallize in between the first block's lamella. This template creates spatial restriction for the crystallization of the block that crystallizes second. This can sometimes cause less crystallinity of the second block due to confinement effects.[35-36] Additionally, it is possible for interfibrillar or fractional crystallization to occur.[36-38]

Because the first block to nucleate and crystallize determines the final crystal morphology and relative block crystallinity, the contribution of each block's properties in the copolymer can be altered by manipulating the block crystallization

order. Here, casting solvent and film drying temperature were studied to determine the effect on the relative block crystallinity and morphology of PEO-*b*-PCL films of varying $w_{PCL}$. Samples were analyzed using FTIR and POM to determine the robustness of crystal structure manipulation using different film preparation conditions. Compositions ranging from $w_{PCL}$ = 0.50 – 0.83 were studied. Relative crystallinity and film morphology varied using chloroform, toluene, and tetrahydrofuran (THF) as casting solvents due to differences in PEO or PCL solubility.

## EXPERIMENTAL

### Materials

PEO-*b*-PCL samples of varying PCL weight fraction were analyzed. A list of samples is shown in Table 1, where the naming shorthand 5k5k represents the molecular weight in g·mol$^{-1}$ of each block, respectively. Samples were purchased from Polymer Source, Inc. and Advanced Polymer Materials, as denoted in Table 1, and used as received. Molecular characteristics were confirmed using $^1$H NMR. Chloroform and THF were obtained from EMD Millipore Corporation, and toluene was purchased from Fisher Scientific International, Inc. THF was distilled to ensure dryness. KBr salt plates used for FTIR analysis were purchased from International Crystal Labs.

TABLE 1 PEO-*b*-PCL Sample Characteristics

| Sample | $M_n^{PEO}$ (g mol$^{-1}$) | $M_n^{PCL}$ (g mol$^{-1}$) | PDI | $w_{PCL}$ |
|---|---|---|---|---|
| 5k5k[a] | 5000 | 5000 | 1.18 | 0.50 |
| 5k10k[b] | 5000 | 10000 | 1.17 | 0.67 |
| 5k16.3k[a] | 5000 | 16300 | 1.40 | 0.76 |
| 5k24.5k[a] | 5000 | 24500 | 1.30 | 0.83 |

[a] Polymer Source, Inc. [b] Advanced Polymer Materials

### Differential Scanning Calorimetry (DSC)

DSC analysis was performed using a PerkinElmer DSC 8000 paired with an Intracooler 2. 3.0 to 5.0 mg of each sample was loaded into a standard aluminum DSC sample pan. Difference in mass between sample pan and reference pan was less than 0.1 mg. Samples were heated to 80°C, held for 5 minutes, and then cooled to -20°C at a rate of 10°C min$^{-1}$ to observe the crystallization behavior.

### FTIR Analysis

1% (wt/wt) solutions were created by dissolving powder polymer samples in chloroform, toluene, or THF at room temperature or with slight heating to ensure dissolution. Prepared solutions and KBr salt plates were incubated in an oven at the desired drying/crystallization temperature for 10 minutes to ensure temperature equilibration before casting. 200 μL of the solution was drop cast onto the KBr salt plate. The solvent was allowed to evaporate in the oven at various temperatures ($T_{iso}$) for one to ten hours. Melt films were drop cast from chloroform and put into a separate oven at 80°C for 10 minutes to melt the film and remove any solvent effects before placing into the oven at $T_{iso}$. After the drying time had concluded, the KBr salt plates were allowed to cool to room temperature and films were analyzed using a Thermo Fisher Scientific Nicolet 6700 FTIR[39] in transmission mode. ATR-FTIR using a single-bounce diamond crystal was performed on THF-polymer solutions. The solution was drop cast onto the crystal, and spectra were collected during drying. All FTIR data was collected as 8 scans with a data spacing of 0.964 cm$^{-1}$

(resolution of 16), which allowed for fast collection and well-averaged spectra.

**Polarized Optical Microscopy (POM)**

200 μL of each prepared 1% PEO-*b*-PCL solution was drop cast onto a glass slide and allowed to dry. A Leica DM2700P POM with a CCD camera attachment was used to analyze prepared samples. Visualization of different morphologies was enhanced by using a quarter-wave plate. A Mettler Toledo HS82 hot stage was used to prepare melt-recrystallized films.

**RESULTS**

Our previous work[21] demonstrated that the choice of solvent influenced the crystallization sequence in equal molecular weight PEO-*b*-PCL films. In this paper, the role of $w_{PCL}$ and solvent choice was evaluated to determine their role in the final relative crystalline content and, in a related way, the crystal morphologies. At higher $w_{PCL}$, the large PCL component should dominate and control the crystallization behavior, regardless of solvent.

**DSC Results**

DSC cooling experiments were performed on as-received polymer powder to determine the relative onset non-isothermal crystallization temperatures ($T_x$). This indicated whether both blocks should crystallize at ambient conditions during film preparation. The cooling thermograms for 5k5k, 5k10k, 5k16.3k, and 5k24.5k PEO-*b*-PCL are shown in Figure 1. The first peak is assigned to PCL crystallization because of its larger weight fraction,[17-18,21,23-35] and therefore the second peak (indicated by arrows) was assigned to PEO crystallization. Onset $T_x$s were determined for both PCL and PEO using Pyris software. Specifically, a tangent line was drawn from the inflection point of the curve (or near in some PEO cases) to the baseline. The intersection of the tangent and baseline was considered the $T_x$-value. Table 2 is a summary of the $T_x$s of each block in each sample. 5k5k produced one peak with a small shoulder, which is a superposition of each block's crystallization peak, indicating one coincident crystallization event. The shoulder is a result of the delay in PEO's onset crystallization when compared with PCL, though the shoulder is difficult to assign as purely PEO given the complex crystallization mechanism.[28] Because of this complicated mechanism, the same $T_x$ has been assigned to PEO and PCL in Table 2.

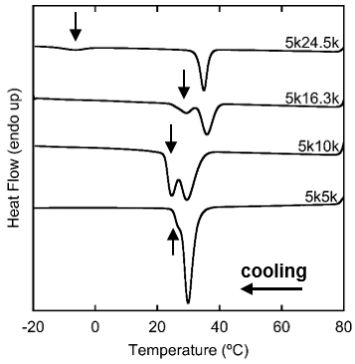


FIGURE 1 DSC cooling thermograms of 5k5k, 5k10k, 5k16.3k, and 5k24.5k samples from 80°C (melt) to -20°C at 10°C min$^{-1}$. Arrow indicates crystallization of the PEO block.

TABLE 2 Onset Crystallization Temperatures for PEO and PCL Blocks

| Sample | $T_x^{PCL}$ (°C) | $T_x^{PEO}$ (°C) |
|---|---|---|
| 5k5k | 32.0 | 32.0 |
| 5k10k | 34.5 | 29.6 |

| | | |
|---|---|---|
| 5k16.3k | 39.4 | 33.4 |
| 5k24.5k | 37.0 | -1.0 |

The 5k10k, 5k16.3k, and 5k24.5k DSC thermograms in Figure 1 contain two distinct peaks indicating two separate crystallization events, or a sequential crystallization mechanism. Here, the sample had to be further cooled for the PEO block to begin crystallizing. This mechanism allowed the first crystallizing block, PCL, to have more of an influence on the macroscopic structure and relative block crystallinity because it was allowed to finish or nearly finish crystallizing before the second block could begin (dependent on cooling rate), resulting in more spatial confinement of the second block. For example, at $w_{PCL}$ = 0.83, the $T_x^{PEO}$ was depressed significantly to -1°C, which may indicate a fractionated crystallization as seen by Müller and coworkers.[36,38] Since these experiments were performed non-isothermally, the two peak areas for moderate $w_{PCL}$ still overlapped. With the complex nature of coincident crystallization for comparable weight fractions, the role of the non-crystallizing block as a diluent is complicated since both components prefer to nucleate competitively. With an increase in $w_{PCL}$, $T_x^{PCL}$ increased slightly to indicate a true separation of the two blocks' nucleation and growth. $T_x^{PCL}$s were lower than homopolymer PCL due to small diluent contributions. The overlap of PEO and PCL crystallization for 5k16.3k likely was due to the larger polydispersity (1.40) compared to most other samples with similar $w_{PCL}$.[17-18] 5k24.5k was the only sample without PEO crystallization at ambient temperature, further supporting that conditions for film preparation should have no effect on relative crystallinity and minimal effect on crystal/film morphology at high $w_{PCL}$.

**Relative Block Crystallinity**

FTIR and POM were used to evaluate the crystallization in PEO-*b*-PCL films. FTIR was used to identify the relative crystalline content rather than a more typical DSC approach because the significant overlap in crystallization peaks made a quantitative analysis cumbersome, though this approach is still under investigation. The high possibility of melt-recrystallization during heating further complicates an effective quantitative analysis by DSC. Additionally, assignments of melting events during heating of the film would be reliant on another form of analysis, such as FTIR or WAXD, anyway. Since the FTIR absorbance of crystalline chains is proportional to the crystalline amount, a qualitative comparison using this single FTIR technique was chosen. POM provided morphological evidence to support the relative crystallinity exhibited by the FTIR study.

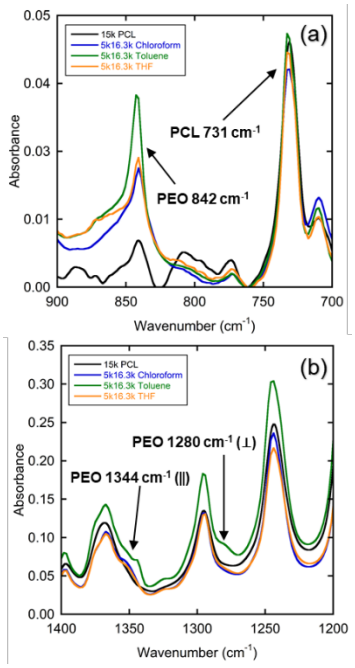

FIGURE 2 Overlaid FTIR spectra of 5k16.3k cast from chloroform (blue line), toluene (green line), THF (orange line), and 15k PCL homopolymer cast from chloroform (black line) with relevant PEO and PCL crystalline peaks labeled. (a) FTIR range of 700 – 900 $cm^{-1}$. (b) FTIR range of 1200 – 1400 $cm^{-1}$. Parallel and perpendicular vibrations are labelled.

Each block has a set of FTIR bands associated with its crystalline and its amorphous forms (see for example Refs. 40-42). The most comparable and deconvoluted set of peaks for determining relative crystallinity were 842 $cm^{-1}$ ($CH_2$ rocking) for PEO and 731 $cm^{-1}$ ($CH_2$ rocking) for PCL. These bands correlate to coupled, resonant motion in two consecutive $CH_2$ groups and five consecutive $CH_2$ groups, respectively.[43] Because PCL chains have the potential for vibrational coupling of two adjacent $CH_2$ groups, either in the crystalline chain or in the rigid amorphous fraction, it was important to verify any PCL contribution to absorption at the 842 $cm^{-1}$ band at large $w_{PCL}$. Figure 2a shows FTIR spectra of as-cast films of 5k16.3k from different solvents and of 15k PCL homopolymer. In 5k16.3k ($w_{PCL}$ = 0.76) films cast from toluene (green line), a large absorbance was observed at 842 $cm^{-1}$. This was attributed to crystalline PEO as this signal matches well with all previously reported data. However, homopolymer PCL (black line) does have a small absorption at 842 $cm^{-1}$. This result shows that the crystalline PCL could contribute to the 842 $cm^{-1}$ band. The $w_{PCL}$ = 0.76 sample cast from chloroform (blue line) and THF (orange line) shows a similarly small absorbance. The small absorbance can be assigned to both the crystalline PCL component and crystalline PEO by comparison to the three other spectra. Reasons for the difference in crystallization behavior with different solvent will be discussed later.

When the PEO component of 5k16.3k was crystallized, the signal from PEO was dominant, making identification of PEO crystallization somewhat obvious, and indicating that even with small PEO composition ($w_{PEO}$ = 0.24), the PCL absorbance at 842 $cm^{-1}$ was markedly less significant. Figure 2b shows FTIR spectra for the same samples at higher wavenumber. This data was used to identify further whether PEO crystals were formed. The presence of bands at 1280 $cm^{-1}$ ($CH_2$ twist perpendicular to the chain axis), 1344 $cm^{-1}$ (PEO $CH_2$ wag parallel to chain stem axis), and/or 1361 $cm^{-1}$ (PEO $CH_2$ wag perpendicular to chain stem axis) confirm PEO crystallization in chloroform and toluene but not THF.[22,40] PCL absorbs at 1295 $cm^{-1}$ (C-O stretch parallel to the chain stem axis) and 1367 $cm^{-1}$ ($CH_2$ wag parallel to the chain stem axis) which overlap with the PEO absorbances; therefore, only small peaks were observed which are denoted by arrows in Figure 2b.

Because crystalline PCL contributes a small absorbance at 842 $cm^{-1}$, it complicated the approach of comparing the two absorbance values at 842 and 731 $cm^{-1}$ to determine relative crystallinity. In most cases, the 842 $cm^{-1}$ band is a superposition of both crystalline PEO and a small contribution from PCL. There was typically enough amorphous PEO absorbance from 830-870 $cm^{-1}$ (Figure 2) to cover the PCL signal ($w_{PCL}$ of 0.50 and 0.67). Amorphous PEO has a maximum around 854 $cm^{-1}$. As PCL block length increases, however, it is important to account for this small PCL absorbance because the 842 $cm^{-1}$ band may appear to show crystalline PEO when, in fact, it is completely amorphous.

Relative crystallinity of the blocks, therefore, was described using a (PEO/PCL) ratio of the crystalline band absorbances of each block, $A_{PEO}/A_{PCL}$, for a given sample. Since the

absorbance is proportional to crystalline mass fraction of the irradiated area, this method is semi-quantitative in relation to crystallinity and normalizes against film thickness, though does not account for the changing mass fractions overall. For completely amorphous PEO, a band centered around 854 $cm^{-1}$ was present which can be used as a normalization, because its absorbance does not change with phase changes. To minimize the PCL-produced 842 $cm^{-1}$ absorbance, and to accurately account for only crystalline PEO, the commensurate absorbance at 854 $cm^{-1}$ was subtracted from the absorbance at 842 $cm^{-1}$, following Equation 1:

$$\frac{A_{PEO}}{A_{PCL}} = \frac{A_{842} - A_{854}}{A_{731}} \quad (1)$$

This normalization helps to remove any contribution of amorphous PEO from $A_{842}$; therefore, $A_{PEO}$ should be representative of crystalline PEO only. The 854 $cm^{-1}$ absorbance is synonymous with an isosbestic point because its absorbance does not change significantly with phase changes. There is minimal decrease in absorbance between 852 and 870 $cm^{-1}$; therefore, the 842 $cm^{-1}$ band appearance has been denoted evidence of crystalline PEO.[42] This method provided a quick and easy way to compare crystallization using different samples and different conditions. Two weaknesses of this method, however, are that little to no crystallization of either block causes an artificially high or low absorbance ratio as the numerator or denominator approaches zero and that these values have modest physical meaning without knowledge of the absorptivity constant.

PEO-*b*-PCL films were cast and dried from various solvents and at various $T_{iso}$. The as-cast films were analyzed using transmission FTIR to determine the relative crystallinity of the two blocks. (PEO/PCL) absorbance ratio ($A_{PEO}/A_{PCL}$) as a result of casting from different common solvents was plotted versus $T_{iso}$ in Figure 3. Films cast from chloroform (blue diamonds), toluene (green squares), THF (orange circles), and melt-recrystallized (black triangles) are plotted. It should be noted here that crystallization that occurred during drying at $T_{iso}$ was not distinguished from crystallization that may have occurred during cooling under ambient conditions after removal from the isothermal oven. The absorbance ratio is representative of the prepared film (drying at $T_{iso}$ and cooling to room temperature). DSC results in Figure 1 gave some indication of the crystallization process during drying and cooling. It is assumed that for 5k5k ($w_{PCL}$ = 0.50) PEO-*b*-PCL, both blocks crystallized during drying. For 5k10k ($w_{PCL}$ = 0.67), it was likely that both blocks crystallized during drying. Though, at the highest temperatures, PEO may have remained amorphous until cooling. For 5k16.3k ($w_{PCL}$ = 0.76), it is likely that only PCL crystallized during drying at higher $T_{iso}$, and PEO crystallized during cooling to room temperature based on the $T_x$ observed in DSC. For 5k24.5k ($w_{PCL}$ = 0.83), only PCL crystallized with no PEO crystallization because the films were not quenched below $T_x^{PEO}$ = -1°C.

Several trends are observed in Figure 3. First, as $w_{PCL}$ increased, the absorbance ratio decreased due to restrictions in PEO crystallization with larger PCL content.[17-18,23-24,34] As a reference, since no PEO crystallization occurs in the $w_{PCL}$ = 0.83 sample, an $A_{PEO}/A_{PCL}$ value of approximately 0.20 or less indicates only PCL crystallization. A value greater than zero also supports the observation that a small 842 $cm^{-1}$ peak appeared for PCL crystallization, as discussed above. As seen in Figure 2, 842 $cm^{-1}$ absorption for $w_{PCL}$ = 0.76 was significant to identify PEO

crystallization. This resulted in an $A_{PEO}/A_{PCL}$ ratio between 0.30 and 0.50. Also, it was observed that since PCL is the majority component in most instances here, the 731 $cm^{-1}$ band absorption was nearly constant. These two results seemed to indicate that variation in $A_{PEO}/A_{PCL}$ likely was due to changes in PEO crystallization. Significantly larger ratios in $w_{PCL}$ = 0.50 ($A_{PEO}/A_{PCL}$ > 2.0) compared to $w_{PCL}$ = 0.67 were due to the moderately larger PEO mass fraction, resulting in more absorbing species per volume. The role of molecular weight and weight fraction have been studied extensively elsewhere. This trend only serves as reference for the role of $T_{iso}$ and solvent for each sample.

FIGURE 3 (PEO/PCL) absorbance ratio ($A_{PEO}/A_{PCL}$) as a function of drying temperature ($T_{iso}$) from 30°C to 45°C. (a) $w_{PCL}$ = 0.50, (b) $w_{PCL}$ = 0.67, (c) $w_{PCL}$ = 0.76, (d) $w_{PCL}$ = 0.83. As-cast films from chloroform (blue diamonds), toluene (green squares), THF (orange circles), and films that had been melted and recrystallized (black triangles).

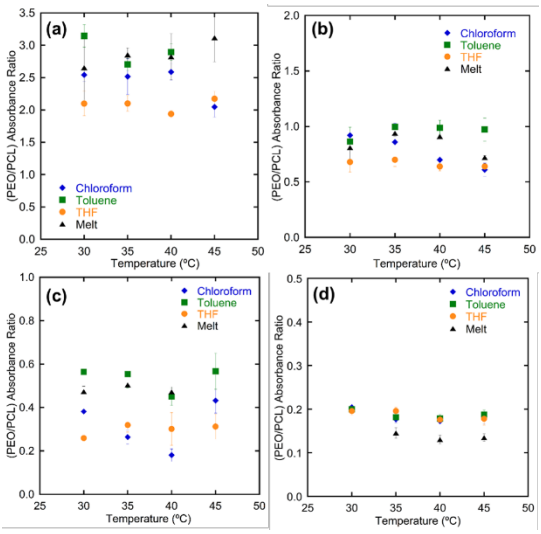


Error bars represent one standard deviation.

Second, $T_{iso}$ had a minimal effect on the final (PEO/PCL) absorbance ratio. Crystallization of the two blocks was competitive for $w_{PCL}$ = 0.50 and 0.67 since both likely crystallized at all $T_{iso}$. For $w_{PCL}$ = 0.83, the ratio remained constant over $T_{iso}$ because PCL was the dominant crystal present. Chloroform was a bit unique in that the ratio decreased slightly with $T_{iso}$ for $w_{PCL}$ = 0.67 and 0.76. Additionally, the crystallinity of PCL remained relatively constant. It is unclear from FTIR only how much the crystallinity changed because there is not an easy way to convert absorbance to crystallinity accurately. Variation in absorbance was likely due to imperfect crystallization due to solvent interactions.

Third, the casting solvent influenced $A_{PEO}/A_{PCL}$ Again, for $w_{PCL}$ = 0.83, sufficient undercooling was needed to nucleate PEO crystallization. It is unsurprising that the solvent does little to promote PEO crystallization at temperatures above -1°C. The melt values are a bit smaller, indicating that the drying process hindered PCL crystallization slightly. Varying $A_{PEO}/A_{PCL}$ values appear for all other $w_{PCL}$ indicating that solvent choice promotes or inhibits PEO crystallization as the minority component. More specifically, films cast from chloroform had ratios between those from the melt and those from THF. Chloroform, therefore, had a slight preference to solubilize PEO. Alternatively, since PCL was the less soluble moiety, chloroform promoted its crystallization first. PCL crystallizes first from the melt due to molecular size. Films cast from toluene (Figure 3, green squares) had higher ratios in nearly all instances. Larger ratios indicate more pronounced PEO crystallization. This was evidence that PEO was less soluble in toluene and perhaps crystallized first. These results match previous research in this area.[22] Interestingly, this effect was observed in films with a $w_{PCL}$ up to 0.76, though the amount of PEO crystallization was small. This may indicate that PCL crystallization was reduced as well giving a

slightly larger $A_{PEO}/A_{PCL}$. THF showed a decrease in the ratio relative to other solvents, indicating that PEO crystallization was underdeveloped in these films. Since THF is a moderately good solvent for PEO, the PEO domains remained more solvated during drying, allowing PCL to crystallize first. While PCL crystallized first for chloroform and melt films, THF restricted PEO crystal formation most. It should be noted here that occasionally THF films had a wet visual appearance, but no measurable FTIR signal for THF at 1066 and 907 $cm^{-1}$ (see Supporting Information, Figure S1). Though the FTIR spectra showed no THF bands, there was on occasion a very small band at 3400 $cm^{-1}$. Since THF is hygroscopic and miscible with water, a small fraction of water could be present. It should be noted that the THF was distilled and stored under dry conditions, and when tested, THF solvent showed no band at 3400 $cm^{-1}$, therefore any water present had accumulated during drying by condensing from humid air. This will be discussed in more detail later. The data in Figure 3 does not include any films that appeared wet.

**Film Morphology**

Crystal morphology of dry films was analyzed via POM. Since $T_{iso}$ seemed to have minimal effect on the relative crystallinity, POM experiments were performed only at room temperature to observe morphology differences in films cast from different solvents. Morphologies at higher $T_{iso}$ were similar, but more pronounced, so they are not presented here. Figure 4 shows the results for each set of sample-solvent combination except 5k24.5k images. As was expected, they showed no difference in film morphology with different solvents but can be viewed in the Supporting Information (Figure S2). Figure 4 is organized by sample 5k5k (a-d), 5k10k (e-h) and 5k16.3k (i-l). In each set, a POM image for a film dried from chloroform, toluene, THF, and melt-recrystallization are included. The sequence is chloroform at the top-left with toluene, melt-crystallization, and THF following around in a clockwise manner.

The melt-recrystallization samples show the typical morphology associated with high nucleation density and small spherulite size of PCL-dominant crystallization, as would be expected.[18,28] Using this as a reference, we looked at the POM images for all other samples in the context of the results shown in Figure 3. In other words, how does the morphology change given the change in relative crystallinity seen in FTIR for the PEO and PCL blocks? The chloroform POM morphology is most similar to melt crystallization. The images in Figures 4a, 4e, and 4i show similar high nucleation density, small spherulite sizes as shown in Figures 4d, 4h, and 4l. The nucleation density during drying was higher from chloroform than the melt-recrystallization sample for two reasons. First, as the solvent is evaporating, the concentration of polymer in solution is increasing, causing local precipitation to occur since chloroform is only a partial non-selective solvent. As drying proceeds, the coalescence of precipitation and crystallization begins to occur in the localized areas, leading to a higher number of nuclei than during melt-recrystallization. Secondly, in the melt-recrystallization process, the sample was quenched to room temperature by removing the melt from the oven. It is likely that nucleation occurs at a higher temperature as the sample cools. This would cause fewer nuclei to form as growth proceeds. Because drying keeps the polymer in the amorphous state at room temperature, the undercooling, or $\Delta T$, driving force is likely more significant and results in more nuclei forming. This could be a manifestation from the evaporation rate and

evaporative cooling as well. These morphologies match well with other reports of PEO-*b*-PCL, where PEO crystallization is not obvious *via* POM but was identified using techniques such as FTIR, XRD, or DSC.[17-18,21,23-34]

Finally, the morphology of films cast from THF was irregular and dependent on $w_{PCL}$. These films' spherulite structures have varying surface coverage, lower nucleation density, and faint birefringence. At highest $w_{PCL}$, the films began to adopt more typical POM morphology and birefringence with still some mild irregularity. Based on the FTIR spectra in Figure 2 (and Figure S1), the crystals that have formed were PCL spherulites, though the PCL crystallinity may be reduced slightly. The 5k5k sample has competitive PEO and PCL coincident crystallization, which appeared to dominate any solvent effects, i.e. the similar block size allowed for local nucleation to occur irrespective of solvent. As $w_{PCL}$ increased, PCL nucleation was favored but residual solvent may have hindered crystal growth and perfection.

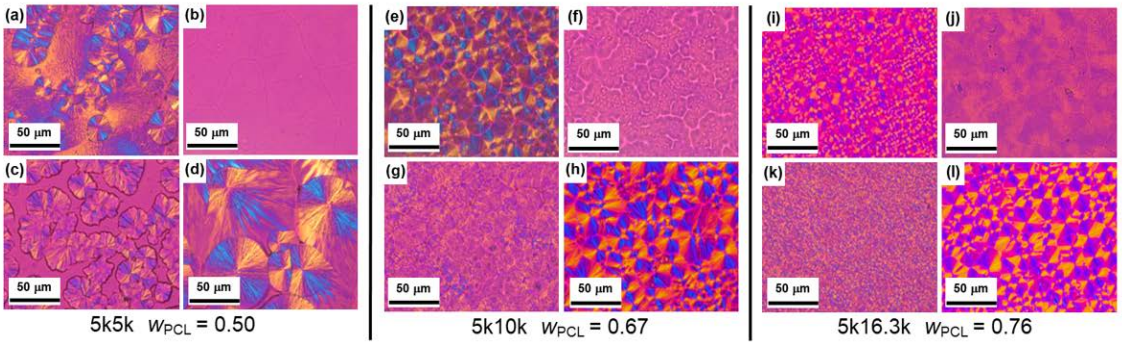


FIGURE 4 POM images of films cast from different solvents: chloroform (a, e, i), toluene (b, f, j), and THF (c, g, k), as well as melt recrystallization (d, h, l) for 5k5k (a-d), 5k10k (e-h), and 5k16.3k (i-l).

Films cast from toluene (Figures 4b, 4f, and 4j) show little-to-no birefringence. Because there is evidence for crystallization of both blocks in the FTIR spectra (Figure 3), it was concluded that crystals in films cast from toluene were preferentially flat-on instead of edge-on. This was supported by our previous findings for 10k10k PEO-*b*-PCL.[22] FTIR spectra confirmed the crystal orientation based on similar analysis of specific bands associated with vibrations parallel to the chain axis (see Supporting Information, Figure S3). The parallel vibrational bands had larger absorption bands in the 5k24.5k sample compared to others indicating that the PEO crystallization is likely important for the flat-on crystal orientation. As $w_{PCL}$ increased, the birefringence became more noticeable, which may indicate a tilting of the crystal axes. However, these spherulites still do not possess the obvious birefringence observed in chloroform and melt-recrystallization films, Figures 4i and 4l, respectively.

Along with the FTIR data, POM shows that the solvent choice impacts the crystallization of the PEO-*b*-PCL copolymer even at moderate $w_{PCL}$. Chloroform morphology appears to follow melt crystallization. Films cast from toluene have a change in crystal orientation for both PCL and PEO crystals. THF hinders the crystallization of PCL by causing irregular morphological development similar to the results seen by

Toolan *et al*.[44] Additionally, the possible solvation of the PEO block by THF or water may hinder PEO crystallization that occurs through ambient drying procedures.

**Role of Humidity in PEO Crystallization**

As mentioned, some films exhibited a wet look after drying indicating the presence of some solvent. These films were not analyzed for the data presented in this article. The presence of incomplete drying did bring up the question: how does the delayed drying affect PEO crystallization? THF and water are both moderately good solvents for PEO. Thus, they would decrease PEO crystallinity as measured by $A_{PEO}$ from the FTIR. For $w_{PCL}$ = 0.50 and $w_{PCL}$ = 0.86, this had minimal influence on the results. For 5k5k, PCL and PEO crystallization happen concurrently with strong tendency for both blocks to nucleate quickly, minimizing the influence of residual THF or water on PEO crystallization. For 5k24.5k, no PEO crystallization occurred at room temperature anyway. For moderate $w_{PCL}$, incomplete drying appeared to prevent PEO crystallization as identified by smaller $A_{PEO}$ and absorbance ratios for the wet-looking films. Interestingly, FTIR absorbance of bands related to THF or water were much smaller relative to the polymer film absorbance. The evaporation process typically takes a slightly longer time than precipitation and crystallization of PCL, allowing PCL to nucleate first, dictating the crystal morphology. It should be noted that PCL has some solubility in THF and minimal water absorption; therefore, the PCL domains may be affected as well but not as significantly because PCL crystallization is more thermodynamically favorable. Given that irregular spherulitic morphologies and significant FTIR absorption at 731 $cm^{-1}$ were observed, PCL crystals formed, confirming that it is less soluble in THF and water than PEO. The swelling of the PEO domains by THF or water is unquantified; therefore, the restrictions on PCL crystallization by the apparent volume fraction of swollen PEO are unknown, though it may be a possible cause for the development of the irregular morphology. The effect on PEO crystallization was most prominent for the 5k10k, $w_{PCL}$ = 0.67 sample.

To evaluate crystallization in films cast from THF more accurately, ATR-FTIR during drying at room temperature was used to evaluate the development of PEO crystallization in the absence of or presence of residual THF/water. Raw ATR-FTIR spectra for the drying of 5k5k, 5k10k, and 5k16.3k films on the diamond ATR crystal are shown in the Supporting Information (Figure S4). The spectra is characteristic of THF at early times. As the THF evaporates, the typical

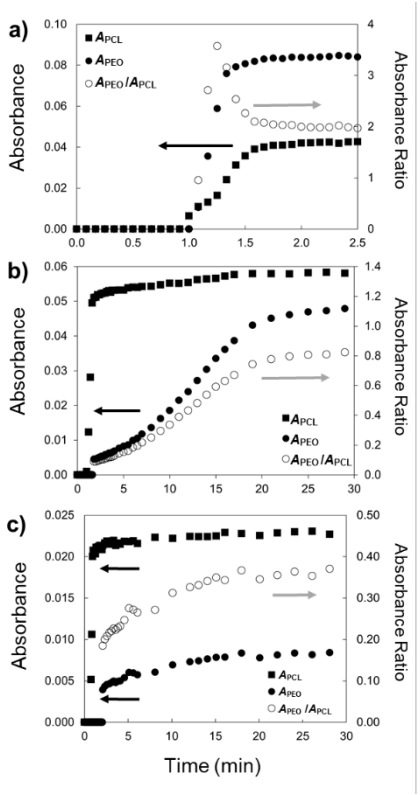

PEO-*b*-PCL spectrum appears. At longer times, the PCL band increases in absorbance and reaches a constant value when PCL primary crystallization has ceased. Eventually, the crystalline PEO band at 842 $cm^{-1}$ begins to appear. At longer times, the PEO band no longer increases, indicating that PEO crystallization has stopped. Figure 5 shows plots of absorbance versus time for the two bands, 731 $cm^{-1}$ ($A_{PCL}$) and 842 $cm^{-1}$ normalized by the absorbance at 854 $cm^{-1}$ as discussed earlier ($A_{PEO}$), and their $A_{PEO}/A_{PCL}$ ratio. Figure 5a shows the plot for 5k5k. Figure 5b is the 5k10k sample under normal conditions. Figure 5c is the plot for 5k16.3k.

From 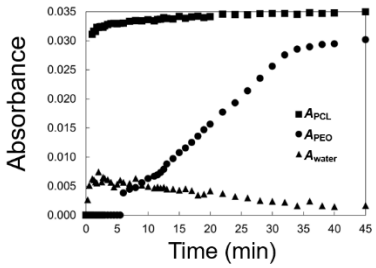

the absorbance versus time plots, it was apparent that for $w_{PCL}$ = 0.50, PEO nucleation occurred simultaneously with PCL nucleation with a faster crystallization rate. For $w_{PCL}$ ≥ 0.50, PEO nucleation is delayed relative to PCL crystallization, though it does occur relatively shortly after for 5k10k and 5k16.3k. These short nucleation times demonstrated minimal inhibition by THF or water under "dry" conditions. In Figures 5b and 5c, $A_{PEO}$ is much smaller due to less PEO crystallinity. This is confirmed by the lower absorbance ratios as shown in Figure 3.

FIGURE 5 $A_{PEO}$ and $A_{PCL}$ as a function of drying time from THF solution: (a) 5k5k, (b) 5k10k, and (c) 5k16.3k. Absorbance ratio ($A_{PEO}/A_{PCL}$) as a function of time plotted on secondary y-axis.

For a film with residual solvent or a small amount of water, the PEO crystallization was delayed as evidenced by $A_{PEO}$. Figure 6 shows a similar plot of absorbance with drying time for a 5k10k film cast in a humid environment. Figure 6 shows that PCL crystallization occurred quickly, while PEO crystallization was delayed several minutes after the PCL crystallization. In addition, the maximum PEO crystallization was achieved at a later time compared to dry conditions. This delayed PEO crystallization was different than the results shown in Figure 5. Figure 6 also shows the absorbance at 3430 $cm^{-1}$, which is representative of -OH stretching in water ($A_{water}$). A small amount of water that was adsorbed (or absorbed) during evaporation is present early during drying. The mechanism of water infiltration is difficult to understand as the FTIR absorbance was small. As time progresses, this water signal begins to decrease as $A_{PEO}$ increases. The final $A_{PEO}/A_{PCL}$ for these films was 0.85, which is comparable to a completely dry film.

FIGURE 6 $A_{PEO}$, $A_{PCL}$, and $A_{water}$ as a function of drying time for 5k10k ($w_{PCL}$ = 0.67).

In moderately humid conditions, PEO crystallization was delayed up to a few hours. This observation confirmed that the PEO crystallization had been inhibited by the presence of THF (residual solvent or slower evaporation) and water. In highly humid conditions, films appeared wet after drying overnight. It should be noted that the 3430 $cm^{-1}$ band is characteristically large for water. Given the small absorbance seen in Figure 6, the mass of water must be small relative to the mass of PEO-*b*-PCL film. Again, no THF bands were observed, but with significant overlap with PEO and PCL bands, a residual amount cannot be

negated. This was true even in the higher humidity situations. Absorbance ratios for films with inhibited PEO crystallization were near 0.40 with a small $A_{water}$. These films were dried in vacuum. After removal of water *via* this method, the absorbance ratio became comparable to the values reported for dry films, ~0.80.

## DISCUSSION

This study evaluated the role of casting solvent and drying temperature on PEO-*b*-PCL copolymer films with varying PCL content. From the results, the two processing parameters influenced the crystallization order for low $w_{PCL}$ and had little-to-no effect at highest $w_{PCL}$. Low $w_{PCL}$ films (5k5k, $w_{PCL}$ = 0.50) were shown to have coincident, or nearly coincident, crystallization mechanisms. As such, the nucleation barrier between the two components was more similar. As $w_{PCL}$ increased, the crystallization mechanism was driven by the larger PCL block. PEO crystallization was limited because it is the minority component. Casting solvent and drying temperature did not change significantly the thermodynamics of the system; therefore, PEO crystallinity and film morphology were consistent at the highest $w_{PCL}$.

Slight changes to the casting conditions have a greater impact on the 5k5k ($w_{PCL}$ = 0.50) sample because of the similar nucleation barrier of each block. Preferential solvation of one block over the other, toluene/PCL and THF/PEO, induces changes in final crystallinity. $A_{PEO}/A_{PCL}$ was much larger for toluene than for THF, PEO crystallized more significantly. Solvent effects on crystallization became less influential as the block asymmetry increased because diluent effects on the PEO minority block dominated PEO crystallinity more than solvent effects. As an example, POM images in toluene showed that as the $w_{PCL}$ increased, edge-on crystals formed, and $A_{PEO}/A_{PCL}$ absorbance ratios from FTIR data became increasingly similar. Because PCL dominated crystallization so heavily and crystallized so much in the time given, $A_{PEO}/A_{PCL}$ absorbance ratios were very small due to a large denominator in addition to a small numerator caused by low crystallization of PEO. Large block asymmetry allows PCL to crystallize similar to its homopolymer regardless of solvent, and PEO crystallization occurs only at large undercooling.

When the crystallization was manipulated, the measured FTIR absorbance and the film's spherulitic morphology showed that PEO crystallization was impacted most. If PEO crystallized first or PCL was more solvated in the toluene-cast films, $A_{PEO}/A_{PCL}$ increased. This showed that PEO had a higher crystallinity than in films casted from other solvents. Flat-on crystal morphology was more prevalent in POM images for toluene cast films, which was evidence that PEO may have nucleated first in the film. Solvent quality for the PCL block helped determine the spherulitic morphology because crystallization during drying is poorer in good solvent. POM images showed more irregular spherulites in toluene/THF for this reason. In THF-cast films, PCL nucleated and crystallized first, similar to chloroform and melt; however, the interaction of PEO and THF (or water in some instances) delayed PEO crystallization. This interaction decreased the PEO crystallinity compared to films cast from other solvents. Most interesting was that when PEO crystallization was delayed significantly by water adsorption for the 5k10k, $w_{PCL}$ = 0.67 sample, the final absorbance ratio after complete removal of residual solvent was comparable to dry THF conditions. This indicates that after removal of residual THF and/or water, the PEO reached a similar crystallinity. Assuming PCL maximized

crystallinity while PEO remained amorphous, this showed that PCL crystallinity at room temperature has minimal influence on PEO crystallinity. In other words, the PEO crystallization process appeared unhindered by formation of PCL crystals, only by residual solvent. This appeared to be true for films dried at higher $T_{iso}$ as well. Since $T_x^{PEO}$ was near 30°C and slightly lower than $T_x^{PCL}$, PEO crystallization occurred after PCL. However, there was only a small decrease of the absorbance ratio at higher $T_{iso}$ for $w_{PCL} \geq 0.67$.

Solubility of each block in the chosen casting solvent is a major driving force for relative block crystallinity differences. This is two-fold: 1) relative solubility based on Flory-Huggins interaction parameter of polymer with solvent, $\chi_{P\text{-}S}$ and 2) the relationship between $\chi_{PEO\text{-}S}$ and $\chi_{PCL\text{-}S}$ and temperature, which should be inequivalent for the two blocks. Our previous work demonstrated the crystallization order switch in solvents with varying solubility parameter.[21] In the examples here, there was no obvious switching in crystallization order with $T_{iso}$ (perhaps at high $T_{iso}$ for $w_{PCL}$ = 0.50 though not obvious here). This is evidence that the change in solubility of each block with temperature appears to be comparable or that the influence of solubility on crystallization does not appear to change with temperature under these conditions. Chloroform films showed that PEO likely became a bit more soluble as $T_{iso}$ increased - indicated by the decreasing absorbance ratio. Additionally, It should be noted that the vapor pressure of the solvent increases with $T_{iso}$. This should decrease the solvent's residence time in the film, though partially dependent on the magnitude of $\chi_{P\text{-}S}$. At higher $T_{iso}$, solubility effects could be reduced due to faster evaporation rates. When the solvent's residence time in the film decreases, the crystallization may more closely follow that of the melt.

Unfortunately, the thermodynamics for drying and crystallization in these films are quite complicated and convoluted. Crystallization likely is controlled by $\chi_{P\text{-}S}$, $\chi_{P\text{-}S}(T)$, isothermal crystallization kinetics, diluent effects, confinement effects, morphology, surface or interface interactions, and evaporation rate. Identifying the role of each individual factor is difficult because of this connectivity. Our approach was from the practical side of identifying differences in crystallization and crystallinity as a function of fabrication conditions. Our results show that solvent choice, drying temperature, and molecular weight are important factors in tailoring crystallization in PEO-*b*-PCL films. These results support our previous results comparing crystallization order and solubility parameters.[21]

## CONCLUSIONS

PEO-*b*-PCL films with varying $w_{PCL}$ have been shown to exhibit different crystallization behavior based on film preparation techniques. Films were dried from chloroform, toluene, and THF at different isothermal temperatures. FTIR analysis showed that the amount of PEO crystallization was influenced by the choice of solvent. Toluene increased the PEO crystallinity; THF decreased the overall crystallinity; and chloroform crystallinity varied with $T_{iso}$ and $w_{PCL}$. Isothermal drying temperature was shown to have minimal effect on the crystallinity of PEO-*b*-PCL films. Additionally, POM morphology of the crystals showed evidence of strong PCL spherulitic crystallization in chloroform. Toluene exhibited flat-on crystallization with diminished birefringence. Films dried from THF showed an irregular crystal morphology due to the role of

adsorbed water from the humid laboratory environment. This phenomenon could be overcome through complete removal of water and/or THF by vacuum drying. For all observed relative crystallinities and morphologies, the solvent effect diminished as $w_{PCL}$ increased.

These studies show that the solvation of one of the blocks during drying hinders crystallization while the first block nucleates and grows during or after evaporation. This was especially apparent for the $w_{PCL}$ = 0.67 sample where residual solvent suppressed PEO crystallization. PCL was able to crystallize for an extended time because of this suppression; however, final PEO crystallization was seemingly unaffected. Solvent effects on the crystallization of the polymer stem from the different solubility of each block in the chosen solvent. The relationship among precipitation, nucleation and crystal growth, and solvent evaporation rate is critical in determining how block crystallinity progresses. As block weight asymmetry increases, the potential for solvent to influence the crystallization order is reduced since the nucleation barrier of the minority component was greatly increased.

**ACKNOWLEDGEMENTS**

The authors would like to thank the National Science Foundation for support of this project (DMR-1606532 and transfer DMR-1839762).

**REFERENCES AND NOTES**

1. B. N. Sathy, U. Mony, D. Menon, V. K. Baskaran, A. G. Mikos, and S. Nair, *Tissue Eng. Part A* **2015**, *21*, 2480.
2. G. Chandrashekar and N. Udupa, *J. Pharm. Pharmacol.* **1996**, *48*, 669.
3. W. B. Liechty, D. R. Kryscio, B. V. Slaughter, and N. A. Peppas, *Annu. Rev. Chem. Biomol. Eng.* **2010**, *1*, 149.
4. M. L. Adams, A. Lavasanifar, and S. G. Kwon, *J Pharm Sci* **2003**, *92*, 1343.
5. B. Jeong, Y. H. Bae, D. S. Lee, and S. W. Kim, *Nature* **1997**, *388*, 860.
6. M. A. Woodruff and D. W. Hutmacher, *Prog. Polym. Sci.* **2010**, *35*, 1217.
7. M. I. Sabir, X. Xu, and L. Li, *J. Mater. Sci.* **2009**, *44*, 5713.
8. M. C. Serrano, R. Pagani, M. Vallet-Regí, J. Peña, A. Rámila, I. Izquierdo, and M. T. Portolés, *Biomaterials* **2004**, *25*, 5603.
9. Z. Gan, Q. Liang, J. Zhang, and X. Jing, *Polym. Degrad. Stab.* **1997**, *56*, 209.
10. S. Li, H. Garreau, B. Pauvert, J. McGrath, A. Toniolo, and M. Vert, *Biomacromolecules* **2002**, *3*, 525.
11. J. Z. Bei, J. M. Li, Z. F. Wang, J. C. Le, and S. G. Wang, *Polym. Adv. Technol.* **1997**, *8*, 693.
12. R. V. Castillo and A. J. Müller, *Prog. Polym. Sci.* **2009**, *34*, 516.
13. W.-N. He and J.-T. Xu, *Prog. Polym. Sci.* **2012**, *37*, 1350.
14. R. M. Van Horn, M. R. Steffen, and D. O'Connor, *Polymer Crystallization* **2018**, *1*, e10039.
15. C. G. Pitt, In Biodegradable Polymers as Drug Delivery Systems; M. Chasin, R. Langer, Eds.; Marcel Dekker, Inc: New York; 1990.
16. Y. Hou, J. Chen, P. Sun, Z. Gan, and G. Zhang, *Polymer* **2008**, *48*, 6348.
17. C. He, J. Sun, C. Deng, T. Zhao, M. Deng, X. Chen, and X. Jing, *Biomacromolecules* **2004**, *5*, 2042.
18. C. He, J. Sun, J. Ma, X. Chen, and X. Jing, *Biomacromolecules* **2006**, *7*, 3482.
19. J. Albuerne, L. Márquez, A. J. Müller, J.-M. Raquez, P. Degée, P. Dubois, V.

Castelletto, and I. W. Hamley, *Macromolecules* **2003**, *36*, 1633.
20. S. Nojima, Y. Fukagawa, and H. Ikeda, *Macromolecules* **2009**, *42*, 9515.
21. N. Brigham, C. Nardi, A. Carandang, K. Allen, and R. M. Van Horn, *Macromolecules* **2017**, *50*, 8996.
22. R. M. Van Horn, J. X. Zheng, H.-J. Sun, M.-S. Hsiao, W.-B. Zhang, X. Dong, J. Xu, E. L. Thomas, B. Lotz, and S. Z. D. Cheng, *Macromolecules*, **2010**, *43*, 6113.
23. R. Perret, and A. Skoulios, *Die Makromol. Chem.* **1972**, *162,* 147.
24. Z. Gan, B. Jiang, and J. Zhang, *J. Appl. Polym. Sci.* **1996**, *59*, 961
25. B. Bogdanov, A. Vidts, E. Schacht, and H. Berghmans, *Macromolecules* **1999**, *32*, 726.
26. T. Shiomi, K. Imai, K. Takenaka, H. Takeshita, H. Hayashi, and Y. Tezuka, *Polymer* **2001**, *42*, 3233.
27. S. Jiang, C. He, L. An, X. Chen, and B. Jiang, *Macromol. Chem. Phys.* **2004**, *205*, 2229.
28. C. He, J. Sun, T. Zhao, Z. Hong, X. Zhuang, X. Chen, and X. Jing, *Biomacromolecules* **2006**, *7*, 252.
29. J. Yu and P. Wu, *Polymer* **2007**, *48*, 3477.
30. Z.-X. Du, Y. Yang, Y. J.-T. Xu, and Z. Q. Fan, *J. Appl. Polym. Sci.* **2007**, *104*, 2986.
31. Y. Xu, Y. Zhang, Z. Fan, and S. Li, *J. Polym. Sci.: Part B: Polym. Phys.* **2010**, *48*, 286.
32. S. Cometa, F. Chiellini, I. Bartolozzi, E. Chiellini, E. De Giglio, and L. Sabbatini, *Macromol. Biosci.* **2010**, *10*, 317.
33. J. Zhao, J. Zhang, X. Duan, Z. Peng, and S. Wang, *Polymer* **2011**, *52*, 2085.
34. Y. Suzuki, H. Duran, M. Seinhart, H.-J. Butt, and G. Floudas, *Macromolecules* **2014**, *47*, 1793.
35. C. Yu, Q. Xie, Y. Bao, G. Shan, and P. Pan, *Crystals* **2017**, *7*, 147
36. A. J. Müller, V. Balsamo, M. L. Arnal, T. Jakob, H. Schmalz, and V. Abetz, *Macromolecules* **2002**, *35*, 3048.
37. M. Weng and Z. Qiu, *Macromolecules*, **2014**, *47*, 8351.
38. M. L. Arnal, V. Balsamo, F. López-Carrasquero, J. Contreras, M. Carrillo, H. Schmalz, V. Abetz, E. Laredo, and A. J. Müller, *Macromolecules* **2001**, *34*, 7973.
39. While a majority of the experiments were performed at Allegheny College using the Nicolet 6700, a few samples were analyzed using the Thermo Fisher Scientific Nicolet iS50 FTIR at Lafayette College.
40. Y. Zheng, M. L. Bruening, and G.L. Baker, *Macromolecules* **2007**, *40*, 8212.
41. D. Keroack, Y. Zhao, and R. E. Prud'homme, *Polymer* **1999**, *40*, 243.
42. C. Yan, H. Li, J. Zhang, Y. Ozaki, D. Shen, D. Yan, A.-C. Shi, and S. Yan, *Macromolecules* **2006**, *39*, 8041.
43. J. L. Koenig, *Spectroscopy of Polymers*, 2nd Ed.; Elsevier: New York, **1999**
44. D. T. W. Toolan, A. Isakova, R. Hodgkinson, N. Reeves-McLaren, O. S. Hammond, K. J. Edler, W. H. Briscoe, T. Arnold, T. Gough, P. D. Topham, and J. R. Howse, *Macromolecules* **2016**, 49, 4579.
45. S. Jiang, C. He, L. An, X. Chen, and B. Jiang, *Macromol. Chem. Phys.* **2004**, *205*, 2229.

**GRAPHICAL ABSTRACT**

COLE W. TOWER, KRISTI ALLEN, ALLISON CARANDANG, AND RYAN M. VAN HORN

SOLUBILITY CONSIDERATIONS IN RELATIVE BLOCK CRYSTALLIZATION AND MORPHOLOGY OF PEO-*b*-PCL FILMS

TEXT ((up to 75 words, not the same as the abstract text, present tense, no personal pronouns, written for a non-specialist, see recent issue for examples))

Crystallization in polymers is a physical property that has strong influence on other engineering properties, such as strength and degradation rate. This research shows that crystallization in copolymer films with two types of crystals is manipulated by film fabrication conditions, namely casting solvent and drying temperature. Control over the crystallization process allows for control over macroscopic properties.

GRAPHICAL ABSTRACT FIGURE ((Please provide a square image to be produced at 50 mm wide by 50 mm high. Please avoid graphs and other figures with fine detail due to the relatively small size of this image.))